Journal of Magnetic Resonance **147,** 1–8 (2000)
doi:10.1006/jmre.2000.2131, available online at http://www.idealibrary.com on IDEAL®

Protein Hydration and Location of Water Molecules in Oxidized Horse Heart Cytochrome c by ^{1}H NMR

Ivano Bertini,* J. Gaspard Huber,* Claudio Luchinat,† and Mario Piccioli*

**Magnetic Resonance Center (CERM) and Department of Chemistry, University of Florence, Via Luigi Sacconi 6, 50019 Sesto Fiorentino, Florence, Italy; and †Magnetic Resonance Center (CERM) and Department of Agricultural Biotechnology, University of Florence, Florence, Italy*

E-mail: bertini@cerm.unifi.it

Received October 8, 1999; revised May 22, 2000

The hydration properties of the oxidized form of horse heart cytochrome c have been studied by ^{1}H NMR spectroscopy. Two-dimensional, homonuclear ePHOGSY-NOESY experiments are used to map water–protein interactions. The detected NOEs reveal interactions between nonexchangeable protein protons and both water protons and labile protein protons which exchange with water protons. Among the many water molecules apparent in the X-ray structure, three have been identified with a residence time longer than 300 ps. One of them is located inside the distal heme cavity, in the deepest part of a hydration pathway extending toward the surface. The identification of hydrophilic regions and detection of three long-lived water molecules settles some ambiguities and provides a better representation of the water–protein interactions in oxidized cytochrome c. © 2000 Academic Press

Key Words: **paramagnetic systems; heme proteins; protein NMR; water–protein interactions; proton exchange; protein hydrophilicity.**

Water–protein interactions have been extensively discussed with respect to the folding and stability of macromolecules (*1–3*), as well as with respect to protein functions (*4–6*).

A wide range of techniques have been employed to address such interactions, spanning from X-ray (*7*) and neutron diffraction (*8*) to computer simulations (*9, 10*), relaxometry (*11–15*), and high-field NMR spectroscopy (*16–21*). In the latter case, direct interactions of the water molecules with the protein are hardly separated from the interactions mediated through protein protons which exchange with bulk water (*22, 23*). Indeed, water–protein cross-peaks in NOESY- and ROESY-based experiments do not originate exclusively from a direct water–protein nuclear Overhauser effect (NOE) but also from saturation transfer from water to exchangeable protein protons (EP hereafter) and from exchange-relayed NOEs from EP to other protein protons (*17, 18*). To discriminate between direct- and exchange-relayed NOEs, the usual approach is based on the neglect of all NOEs with protons within a 4.0-Å sphere from exchangeable protons (*16, 24, 25*). An alternative experimental approach to reduce exchange-relayed NOEs has been recently proposed, in which resonances of relaying labile protons are quenched through a continuous-wave irradiation (*25*).

We are interested here in the interaction of water with oxidized, paramagnetic, horse heart cytochrome c. This protein has been extensively studied by NMR spectroscopy (*26–29*). The solution structure is reported in both oxidation states (*30–33*), while the X-ray structure is available only for the reduced state (*34*). Information on water–protein interactions is surely relevant in electron-transfer proteins, and suggestions have been made on the role of water in cytochrome c with respect to the reorganization energy associated with electron transfer (*35*). The NMR studies up to now (*4, 30, 36*) have not provided a definite picture of the location and residence time of water molecules inside or around the protein. Part of the difficulty arises from the particularly large number of exchangeable protein protons in horse heart cytochrome c (e.g., the protein contains 19 lysines), which have been shown to be the determinant contributors to water proton relaxation (*37*). Another major problem arises from the fact that the protein is paramagnetic in the oxidized form. Paramagnetism causes fast relaxation close to the metal ion and requires particular attention to minimize loss of information during pulse sequences due to nuclear relaxation.

In order to overcome these problems, we used the ePHOGSY sequence (*38–40*) and adapted it to paramagnetic systems (*36*). The ePHOGSY spectrum reveals dipolar interactions of a proton *i* with water or with a proton exchanging (both slow and fast with respect to the chemical shift separation) with bulk water. Such dipolar interaction is detected through the appearance of NOESY-type cross peaks with nonlabile protein protons. On the above basis, regions of the protein interacting with water on a time scale longer than 300 picoseconds (ps) were identified. The latter time corresponds to the correlation time above which the sign of the NOEs between water protons and protein protons is negative. The sign of saturation transfer is always negative.

Then we separated the effects of direct water protons–protein proton NOEs from the effects due to saturation transfer.

1090-7807/00 $35.00

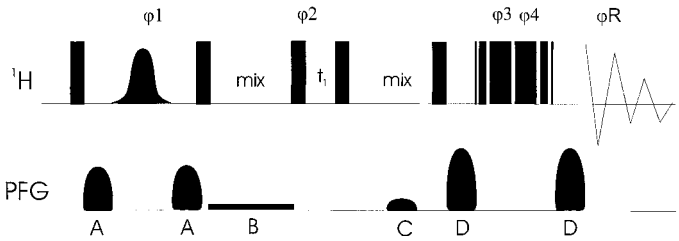

FIG. 1. Pulse sequence used for the ePHOGSY-NOESY experiment (*38*, *39*). The delays were 120 ms for both mixing times, 15 ms for the selective Gaussian pulse, 1.5 s for the recycle delay, and 50 μs for the interpulse delay of the 3–9–19 sequence. Sine-bell-shaped gradients were used, with a length of 864 μs for gradients A and C and of 200 μs for gradient D. Gradient B is a rectangular gradient which was kept for the entire mixing time. Field gradient intensities were 3.0 Gauss/cm for A, 0.2 Gauss/cm for B, 2.3 Gauss/cm for C, and 10.0 Gauss/cm for D. Phase lists (x if not indicated) are as follows: ϕ_1 ($4x$, $4-y$, $4-x$, $4y$), ϕ_2 ($16x$, $16-x$), ϕ_3 ($-x, y, x, -y$), ϕ_4 ($x, -y, -x, y$), ϕ_R ($2(x, -x)$, $2(-x, x)$, $2(x, -x)$, $4(-x, x)$, $2(x, -x)$, $2(-x, x)$, $2(x, -x)$).

In this way we were able to identify three long-lived water molecules associated to the protein.

EXPERIMENTAL PROCEDURES

Sample Preparation

Horse heart cytochrome c (Type VI) was obtained from Sigma Chemical Co. and was used without further purification. The ^{1}H NMR samples were prepared by dissolving the lyophilized protein in 50 mM phosphate buffer adjusted by sodium hydroxyde and hydrochloric acid at a pH value of 5.7, to give 10–15 mM solutions.

NMR Spectroscopy

All experiments were performed at 293 K. The NMR spectra on a sample at pH 5.7 were recorded on a Bruker AMX 600 spectrometer operating at 14.1 T, equipped with a 5-mm probe and a BGU unit for self-shielded z-gradients.

The rationale of ePHOGSY-type experiments and the design of the related pulse sequence has been developed by Dalvit (*38–40*). The sequence used is shown in Fig. 1. This sequence differs only in the final part, after point c, from that previously reported. The classical watergate scheme (*41*), provided by a PFG-90°_{sel}–180°_{nonsel}–90°_{sel}–PFG, which is typically 4–5 ms, has been replaced by a binomial pulse 3–9–19–19–9–3, still sandwiched by two PFGs, with a total duration of 0.7–1.2 ms. This modification turned out to be almost mandatory when dealing with paramagnetic systems. Indeed, it is important to shorten as much as possible the watergate scheme, as the short nuclear relaxation rates may give rise to loss of signals because of T_2 relaxation during the watergate period (*36*). The 3–9–19 pulse permits us to perform a selective 180° pulse within a time which is essentially dependent only on the interpulse delay of the 3–9–19 scheme (*42*). Such time, in the case of large spectral windows, can be as short as a few microseconds. In addition, the length of the two final gradients can be shortened significantly with respect to the usual 1 ms, down to 200 μs, and the recovery time can be shortened down to 150 μs. Both in the standard version and in the present modification of ePHOGSY, water magnetization is invariantly in the xy plane during acquisition, so that demagnetizing field effects are unimportant (*43*).

In all 1D and 2D experiments, a mixing time of 120 ms was used for both water–protein and protein–protein transfer (*38*). The TPPI method was used to obtain quadrature detection in the F1 dimension (*44*). Gaussian shaped, selective 180° pulses of 15 ms were applied on resonance with the carrier frequency at the H_2O position. The recycle delay was 1.5 s. A spectral width of 8400 Hz was used. In the NOESY experiment (*45*), a total of 48 transients were collected for a 2048 $\times$ 870 data point matrix. In the ePHOGSY-NOESY experiment, a total of 640 transients were collected for a 1024 $\times$ 286 data point matrix. Prior to zero-filling (2048 $\times$ 1024 for the NOESY, 1024 $\times$ 512 for the ePHOGSY-NOESY) and Fourier transformation, a squared cosine bell window function was applied in both dimensions. A 1D spectrum, using the same ePHOGSY scheme as before, was recorded as described elsewhere (*36*), as well as the 1D reference spectrum.

One-dimensional CLEANEX-PM (*46*) and two-dimensional CLEANEX-PM-NOESY were collected using a spin lock power of 6.25 kHz. The 1D spectrum was collected using 4096 scans with a delay of 120 ms for the ROESY-NOESY mixing time of the CLEANEX sequence.

A 2D NOESY spectrum was recorded, about one hour after exchange with D_2O, in order to discriminate between exchangeable and nonexchangeable protons in the time scale of one hour (*32*).

All calculations were performed on IBM RISC 6000 computers.

RESULTS

The ePHOGSY-NOESY spectrum on which the present work is based is reported in Fig. 2. An ePHOGSY-NOESY spectrum is a NOESY spectrum displaying cross peaks between proton pairs only if at least one of the two protons is dipole-coupled either to water protons or to exchangeable protein protons (EP). As the mixing process between H_2O (or EP) and protein protons occurs before t_1 evolution of ePHOGSY-NOESY, the intensity of a cross peak A(i, j) in the ePHOGSY-NOESY spectrum is dependent on the NOE of proton i from water (or EP) protons and on the dipole–dipole coupling with proton j. The latter is proportional to the intensity of the A(i, j) cross peak in a reference NOESY spectrum.

To evaluate the ePHOGSY effect, for each cross peak A(i, j) the ratio R_{ij} between the peak volume (V_{ij}) in the

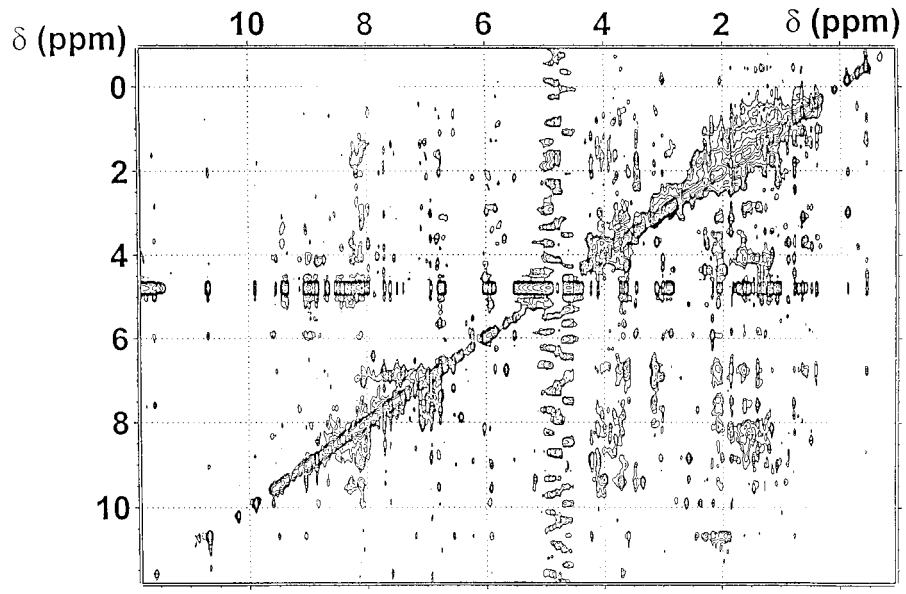

FIG. 2. The ePHOGSY-NOESY spectrum of oxidized horse heart cytochrome c, collected at 600 MHz and 293 K. Conditions are as described under Experimental Procedures.

ePHOGSY-NOESY and that in the reference NOESY experiment is evaluated according to Eq. [1]:

$$R_{ij} = \frac{V_{ij(\text{ePHOGSY-NOESY})}}{V_{ij(\text{NOESY})}}. \qquad [1]$$

The R_{ij} thus depends on the efficiency of the magnetization transfer between water (or EP) and proton i, independently of possible magnetization transfer between water and proton j. As we are dealing with 2D NOESY experiments, more than one R_{ij} ratio in a 2D row may be obtained for each proton i and used to estimate an average R_i ratio for any i proton in the indirect dimension.

A problem in the analysis of ePHOGSY data in terms of protein hydration is related to the selectivity of the 180° selective pulse on the water signal (*38, 39*). Indeed, all the resonances that are excited, completely or partially, by the first 180° selective pulse of the sequence, will originate peaks in the final ePHOGSY-NOESY spectrum. Other experimental approaches have also been proposed to discriminate between intra- and intermolecular NOEs (*47, 48*). To account for this experimental problem, we considered that all the assigned resonances in a ± 180 Hz range from the water resonance (i.e., within the excitation profile of the 15-ms selective pulse on water resonance) are affected by the selective pulse. Additionally, all nonassigned protons of Hα and all the other resonances which are expected to possibly fall in the above range on the basis of the chemical shift index (*49*) were also included in this group of protons. The cross peaks involving protons which are expected, on the basis of the structure, to give rise to dipolar couplings with the above peaks were neglected. After elimination of these possible spurious cross peaks, 114 protons were found from the ePHOGSY-NOESY to experience interactions with water protons or EPs. They are shown in Fig. 3.

To separate the effects of exchange from those of genuine

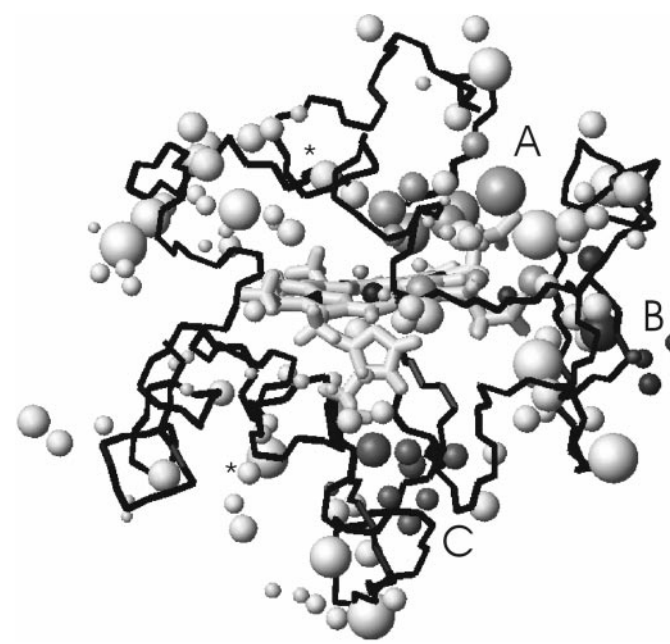

FIG. 3. Hydrophilic map of oxidized horse heart cytochrome c at pH 5.7. Protons are color-coded according to the following criteria: white, surface residue; light gray, region A; dark gray, region B; gray region C; Constraints not belonging to any of the previous regions are indicated with an asterisk. The backbone of the protein is shown as a ribbon. The figure was generated with the program MOLMOL (*64*). The diameter of the spheres reflects the R_i values.

long-lived water protons, we used an approach designed to overestimate the contribution arising from EPs. Indeed, rather than excluding *a priori* all protons being in proximity (typically 4.0 Å sphere (*16*, *24*, *25*)) to an exchangeable proton, we used the solution structure to predict contributions to the observed PHOGSY peaks arising from exchange. This was done by considering the R_i values observed for Hδ and Hϵ protons of tyrosine rings as arising completely from relayed NOEs with OH hydroxyl protons which are in fast exchange with the water molecules and using the tyrosine intraresidue distances as scaling factors. Then, the exchange rates of each EP whose contribution to R_i had to be calculated were estimated as follows:

(i) Peptide NH protons that are unequivocally assigned in a NOESY spectrum of a D_2O-exchanged sample are in very slow exchange with water (exchange rate $<10^{-2}$ s^{-1}). Therefore, despite the fact that they are labile protons, they do not behave like EPs and they are not considered as a source of exchange-relayed NOESY phenomena;

(ii) The exchange rate of EPs that are absent in the D_2O-exchanged sample is estimated from data obtained on small peptides. The exchange rates of backbone amide protons, which can be also experimentally estimated (*50*, *51*), are mostly dependent on the nature of the side chain of the considered residue and of that of the previous one in the primary sequence (*52*). Estimates of exchange rates are also available for exchangeable protons of several side chains (*53*). Using these exchange rates (k_{exc}), the saturation transfer from water to EPs was estimated on the basis of Eq. [2], using an estimated relaxation rate R_1 of 5 s^{-1} for all EPs,

$$\eta = \frac{k_{exc}}{R_1 + k_{exc}}. \qquad [2]$$

(iii) EPs which, on the chemical-shifts time scale, are in fast exchange with water protons will obviously give rise to exchange-relayed NOEs. To account for them, we will treat them as the EPs of the previous group considering a 100% saturation transfer, i.e., $\eta = 1$.

Among the 114 protons detected in PHOGSY experiments and shown in Fig. 3, there are 35 EPs of type (ii), i.e., protons in slow exchange with bulk water. As we are interested in a conservative approach to retain only those peaks that safely arise from water–protein NOEs, we discarded from the 114 protons all of these EPs.

Then, as described above, for the remaining 79 protons we accounted for the contribution of relayed NOEs originating from EPs. This contribution depends on the saturation transfer between water and EPs of types (ii) and (iii). The amount of saturation transfer, given by Eq. [2], is used to scale down the contribution of EPs to each R_i value experimentally obtained.

All *i* protons for which the calculated relayed contributions to the R_i values exceeded 15% were discarded. In order to properly account for the uncertainty in the structure in solution and for the conformational mobility of side chains, the above calculation has been done on each conformer of the family. When the proton *i* was discarded in at least 10% of the 35 conformers, it was not considered as a peak safely arising from water–protein NOEs.

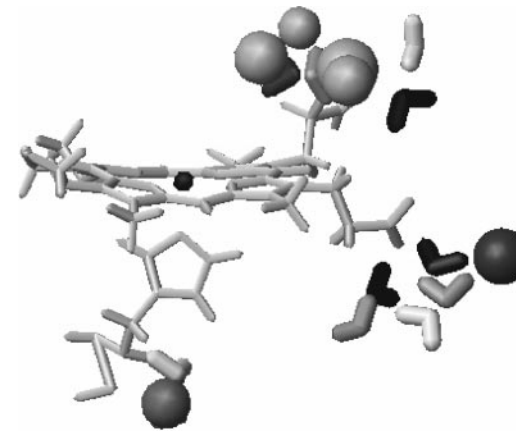

FIG. 4. The six protons identifying the location of long-lived water molecules. They are Trp 59 Hζ_2 and Hη (light gray), Tyr 67 Hβ_2 and Hβ_3 (light gray), Gln 42 HN (dark gray), and Thr 19 HN (gray). Color coding is the same as in Fig. 3. For comparison purposes, the internal water molecules obtained by the different methods are also reported using the following color code: gray, our previous work (*36*); white, NMR previous work (*30*); light gray, X-ray (*56*); black, MD simulation (*55*). The figure was generated with the program MOLMOL (*64*).

The advantage of this approach is that no threshold is required to define the sphere around EPs. Furthermore, the use of the solution structure family somehow accounts for the possible conformational mobility of the lysine residues.

The above approach does not consider fast internal motions of lysine, tyrosine, arginine, threonine, and serine side chains. They may give rise to smaller NOE contributions than main chain amide protons or long-lived water molecules. Furthermore, exchange rates in the protein environment are generally expected to be lower than those measured on small peptides, which we used to estimate the effect of EPs. Therefore, this is a conservative approach that may lead to overestimation of the effects arising from exchangeable protons.

As a consequence of this analysis, a small number of protons is retained whose R_i values surely reflect the presence of a long-lived water molecule nearby. Indeed, the R_i values of only six protons, shown in Fig. 4, were shown to safely originate from water molecules characterized by a residence time longer than the rotational correlation time of the protein. For the above NOEs, corrections due to EPs account for from 2 to 12% of their PHOGSY intensities, thus indicating that they are not close to any EP. This indicates that the six observed NOEs are not biased from our approach. They are, of course, among those that would have been retained using the simple 4-Å threshold (*16*, *24*, *25*).

A complementary experiment has been performed using the

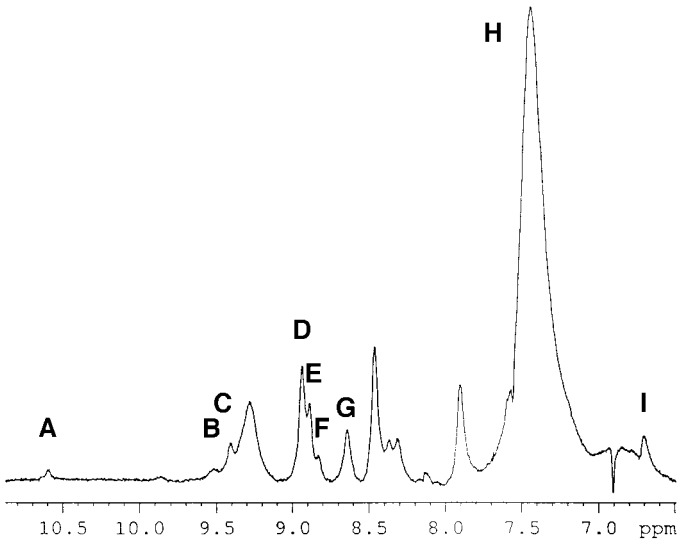

FIG. 5. Down-field part of the 1D CLEANEX-PM spectrum (*46*). A gradient of 0.1 G cm^{-1} was applied throughout the 120-ms mixing time. Peaks are assigned as follows: (A) H_N Glu 61, (B) H_O Thr 78, (C) H_N Gly 23, (D) H_O Tyr 19, (E) H_N Lys 88, (F) H_N His 26, (G) H_N Gly 6, (H) NH_3^+ Lys, (I) $H_{N\epsilon 1}$ Gln 12.

CLEANEX-PM pulse sequence (*46*), which is expected to select only fast exchanging signals. The 1D spectrum is reported in Fig. 5. A strong signal is observed at 7.5 ppm, arising from the NH_3^+ groups of the 19 lysine residues present in the protein. To identify other resonances, we used the CLEANEX-PM sequence as a preparation event for a NOESY-watergate. Such homonuclear 2D experiment turned out to be less sensitive and less informative than a CLEANEX-PM-FHSQC (*54*), but it still permitted the direct identification of some resonances in a nonlabeled sample. In total, the 2D CLEANEX-PM-NOESY provided the assignment of 11 exchangeable protons, 5 being backbone protons (H_N Gly 6, H_N Gly 23, H_N His 26, H_N Glu 61, H_N Lys 88) and 6 belonging to the side chains ($H_{N\epsilon 21}$ and $H_{N\epsilon 22}$ Gln 12, $H_{N\epsilon 21}$ and $H_{N\epsilon 22}$ Gln 16, H_O Tyr 19, H_O Thr 78). In agreement with the prediction, 4 of the 5 backbone protons possess high exchange rates. H_N 61 is well resolved in the 1D CLEANEX-PM spectrum and therefore can be identified despite its relatively small expected exchange rate. The Gln 12 and Gln 16 proton side chains have very intense cross peaks in the NOESY-watergate, thus making possible their identification in the CLEANEX-PM-NOESY. As expected, none of the 6 protons which identify long-lived water molecules is observed in these experiments.

DISCUSSION

Regardless of their origin from direct water–protein NOEs, from saturation transfer on EPs or from intramolecular relayed NOEs originating from EPs experiencing saturation transfer, the 114 protons which are revealed by the PHOGSY experiments provide a picture of those parts of the molecule most in contact with the solvent. Therefore, we will first consider data shown in Fig. 3 and discuss them in terms of "hydrophilic areas," i.e., all the regions that show a high degree of exchange or NOE with water. Then, we will analyze the few peaks which can be safely identified as due to water molecules interacting with a correlation time longer than 300 ps. These few NOEs will not, per se, be capable of locating with precision a long-lived water molecule within the protein. Still, the analysis of these NOEs, together with the data available from X-ray and MD simulation, will allow us to identify the occurrence of three long-lived water molecules and to validate our analysis of hydrophilic areas.

Figure 3 shows the hydrophilic properties of oxidized hh cytc at pH 5.7. There are extended water–protein interactions originating from residues at the protein surface. The observed superficial protein–solvent interactions are not specific, as they are almost distributed over the entire protein surface. Most of these interactions are NOEs relayed from water mediated by the exchangeable protons lying on the protein surface, confirming the efficiency of this mechanism. These superficial protons are indicated in white, in Fig. 3.

On the other hand, the occurrence of internal hydrophilic regions is also apparent. At variance with surface protons, internal "hydrated" protons are not homogeneously distributed. Indeed, a large part of the protein has essentially no internal protons experiencing PHOGSY, while other regions seem to be significantly affected by water–protein interactions. Given the nonhomogeneous distribution of these internal protons, we make the working hypothesis that at least some of them reflect a genuine interaction with an internal water molecule. To better identify these hydration sites, we grouped these internal protons on the basis of their spatial proximity. Three groups could be identified, which are indicated with three different colors in Fig. 3. There are only two protons which are not in spatial proximity with any other internal hydrated proton. They are displayed in white in Fig. 3.

An extended hydrophilic region, which we labeled region A (light gray in Fig. 3), is observed in the distal side of the heme. This relatively large area includes Asn 52, Trp 59, Leu 64, Tyr 67, and Thr 78. The heme itself is also part of this region, as ePHOGSY peaks are observed with one αCH_2 of propionate 7 (*36*). This points to the presence of a hydration pathway in the protein that permits the access of the water down to the heme crevice. It is constituted by the hydrophilic part of the internal residues Asn 52, Tyr 67, and Thr 78. A previous molecular dynamics calculation on both oxidized and reduced yeast cytochrome c predicted the presence of this pathway (*55*). Our result provides experimental evidence for that. This is an important finding to address the electron transfer properties and the dynamics of all cytochromes c.

A second region (region B, dark gray in Fig. 3) is observed, involving residues Gly 41 and Gln 42. This area is located in the so-called proximal half of the protein, but it is almost contiguous to region A.

Another internal region (region C, gray in Fig. 3) still involves the proximal side of the heme and includes the heme-bound Thr 19, Lys 25, Asn 31, and Leu 32.

Figure 4 shows the six protons whose Ri values unambiguously result from intermolecular NOE with a long-lived water molecule using the present conservative approach. Although few, these protons are sufficient to confirm the location of some of the long-lived water molecules that have been previously proposed from X-ray, NMR, and MD calculations (*4, 55, 56*).

Four of these six constraints are in region A (light gray), namely, Trp 59 H_{η} and $H_{\zeta 2}$, and Tyr 67 $H_{\beta 2}$ and $H_{\beta 3}$. These protons are located close to the heme, in the inner part of the hydration pathway. They demonstrate the presence of a water molecule in the heme crevice (the so-called "catalytic" water), with a lifetime of 300 ps or longer, as obtained by the sign of the water–protein NOEs. This is in agreement with all the available X-ray structures of mithocondrial cytochromes c (*5, 34, 56–60*). The position of this water molecule is consistent with our previous proposal (*36*). This molecule could not be identified in earlier NMR work on the oxidized protein (*30*), although it was observed in the reduced protein (*4*). No other conserved NOEs are observed in this region although, as previously discussed, the hydrophilic area A may account for more than one water molecule.

A fifth constraint is located in region B (dark gray sphere), with H_N Gln 42. This constraint is sufficient to show the presence of a long-lived water molecule. Indeed, a water molecule in this region has invariantly been observed from X-ray data about 3.5 Å apart from H_N Gln 42, stabilized by H-bonds with N Gln42, O Lys 39, and an oxygen atom of the heme propionate 7 (*34*).

In most of the available X-ray structures, another internal water molecule is observed close to the water molecule corresponding to region B. No ePHOGSY peak due to NOE or to exchange unambiguously arising from this water molecule has been observed. Therefore, the present results do not provide evidence for the presence of a second long-lived water molecule close to the water of region B.

The sixth NOE is observed in region C with H_N Thr 19 (gray sphere). As in the case of region B, this NOE provides evidence that the identified hydrophilic region also hosts a long-lived water molecule. This is, again, consistent with the available X-ray data on cytochromes c which, in most cases, report the presence of an internal water molecule about 3 Å away from H_N Thr 19, stabilized by H-bonds with Thr 19 and Gly 29.

As no information is available on the chemical shift difference between bulk and protein-associated waters giving rise to exchange-relayed NOEs, no upper limit on the residence time of these waters may be given. Likewise, no information on the lower limit of the residence time of these waters may be given. In the case of BPTI, relaxometry data collected on ^{17}O showed that three of the internal water molecules have residence times in the range 15 ns–1 μs (*61*) while a fourth internal water molecule has a much longer residence time of 0.170 ms (*62*).

It is interesting to compare the present results with a molecular dynamics (MD) study on oxidized yeast cytochrome c (*55*). The MD calculations were run using as the starting point the X-ray structure containing all the crystallographic water molecules and embedded in a bath of ca. 2000 additional waters. The movements of the crystallographic water were followed during the MD trajectory. Only a few waters maintained their approximate position after 200 ps. Among these were the three internal buried waters identified in the present work (regions A, B, and C). Therefore, the MD data support our estimate of the long lifetime of the three water molecules in these regions.

CONCLUSIONS

In this paper we present new experimental evidence for three long-lived water molecules inside the structure of oxidized horse heart cytochrome c, out of the six which were suggested from previous NMR studies (*4, 30*). Unlike the three water molecules identified here, the additional water molecules previously observed by NMR have not been consistently found in the different X-ray structures of oxidized cytochromes c (*63*). All the NOEs which were used in previous papers (*4, 30*) to identify them are also confirmed in the present ePHOGSY-NOESY data, but they are then eliminated, as are many others, when exchange contributions are considered. This indicates that such hydration sites are located in a rather hydrophilic environment, or are relatively external and then accessible to the bulk solvent. Therefore, assuming that the identification of those hydration sites previously pointed out is correct, our data indicate that such water molecules are likely to have much shorter residence times than the three water molecules that we identified with our approach, and therefore, they should not be considered when discussing long-lived water molecules.

ACKNOWLEDGMENTS

Friendly and fruitful discussions with G. Otting are gratefully acknowledged. J.G.H. acknowledges the EU for a post-doctoral fellowship (ERB-CHRX-CT94-0626). This work was supported by CNR, Progetto Finalizzato Biotecnologie, contract 97.01175.49, and by MURST.

REFERENCES

1. J. T. Edsall and H. A. McKenzie, Water and proteins. II: The location and dynamics of water in protein systems and its relation to their stability properties, *Adv. Biophys.* **16,** 53–183 (1983).
2. V. P. Denisov and B. Halle, Protein hydration dynamics in acqueous solution, *Faraday Discuss.* **103,** 227–244 (1996).
3. G. Otting, E. Liepinsh, and K. Wüthrich, Protein hydration in aqueous solution, *Science* **254,** 974–980 (1991).
4. P. X. Qi, J. L. Urbauer, E. J. Fuentes, M. F. Leopold, and A. J. Wand, Structural water in oxidized and reduced horse heart cytochrome c, *Nature Struct. Biol.* **1,** 378–382 (1994).

5. A. M. Berghuis, J. G. Guillemette, G. McLendon, F. Sherman, M. Smith, and G. D. Brayer, The role of conserved internal water molecule and its associated hydrogen bond network in cytochrome c, *J. Mol. Biol.* **236,** 786–799 (1994).
6. Y. Q. Qian, G. Otting, and K. Wüthrich, NMR detection of hydration water in the intermolecular interface of a protein–DNA complex, *J. Am. Chem. Soc.* **115,** 1189–1190 (1993).
7. U. Sreenivasan and P. H. Axelsen, Buried water in homologous serine proteases, *Biochemistry* **31,** 12785–12791 (1992).
8. A. A. Kossiakoff, The application of neutron crystallography to the study of dynamic and hydration properties of proteins, *Annu. Rev. Biochem.* **54,** 1195–1227 (1985).
9. W. F. van Gunsteren, H. J. C. Berendsen, J. Hermans, W. G. Hol, and J. P. Postma, Computer simulation of the dynamics of hydrated protein crystals and its comparison with X-ray data, *Proc. Natl. Acad. Sci. USA* **80,** 4315–4319 (1983).
10. W. F. van Gunsteren and A. E. Mark, On the interpretation of biochemical data by molecular dynamics computer simulation, *Eur. J. Biochem.* **204,** 947–961 (1992).
11. S. H. Koenig and R. D. Brown III, The dynamics of water–protein interactions. Results from measurements of nuclear magnetic relaxation dispersion, *Prog. NMR Spectrosc.* **22,** 487–567 (1991).
12. V. P. Denisov and B. Halle, Dynamics of the internal and external hydration of globular proteins, *J. Am. Chem. Soc.* **116,** 10324–10325 (1994).
13. K. Venu, V. P. Denisov, and B. Halle, Water ^{1}H magnetic relaxation dispersion in protein solutions. A quantitative assessment of internal hydration, proton exchange, and cross-relaxation, *J. Am. Chem. Soc.* **119,** 3122–3134 (1997).
14. V. P. Denisov and B. Halle, Direct observation of calcium-coordinated water in Calbindin D9k by nuclear magnetic relaxation dispersion, *J. Am. Chem. Soc.* **117,** 8456–8465 (1995).
15. I. Bertini, C. Luchinat, G. Mincione, G. Parigi, G. T. Gassner, and D. P. Ballou, NMR studies on *Phtalate Dioxygenase:* Evidence for displacement of water on binding substrate, *JBIC* **1,** 468–475 (1996).
16. G. Otting and K. Wüthrich, Studies of protein hydration in aqueous solution by direct NMR observation in individual protein-bound water molecules, *J. Am. Chem. Soc.* **111,** 1871–1875 (1989).
17. G. Otting and E. Liepinsh, Protein hydration viewed by high-resolution NMR spectroscopy: Implications for magnetic resonance image contrast, *Acc. Chem. Res.* **28,** 171–177 (1995).
18. G. Otting, NMR studies of water bound to biological molecules, *Prog. NMR Spectrosc.* **31,** 259–285 (1997).
19. R. X. Xu, R. P. Meadows, and S. W. Fesik, Heteronuclear 3D studies of water bound to an FK506 binding protein/immunosuppressant complex, *Biochemistry* **32,** 2473–2480 (1993).
20. G. Wider, Technical aspects of NMR spectroscopy with biological macromolecules and studies of hydration in solution, *Prog. NMR Spectrosc.* **32,** 193–275 (1998).
21. A. Mesgarzadeh, S. Pfeiffer, I. Engelke, D. Lassen, and H. Rüterjans, Bound water in apo and holo bovine heart fatty-acid-binding protein determined by heteronuclear NMR spectroscopy, *Eur. J. Biochem.* **251,** 781–786 (1998).
22. G. M. Clore, A. Bax, P. T. Wingfield, and A. M. Gronenborn, Identification and localization of bound internal water in the solution structure of Interleukin 1b by heteronuclear three-dimensional ^{1}H rotating-frame Overhauser ^{15}N–^{1}H multiple quantum coherence NMR spectroscopy, *Biochemistry* **29,** 5671–5676 (1990).
23. G. Otting, E. Liepinsh, B. T. Farmer II, and K. Wüthrich, Protein hydration studied with homonuclear 3D ^{1}H NMR experiments, *J. Biomol. NMR* **1,** 209–215 (1991).
24. K. Wüthrich, G. Otting, and E. Liepinsh, Protein hydration in aqueous solution, *Faraday Discuss.* **93,** 35–45 (1992).
25. G. Melacini, R. Kaptein, and R. Boelens, Editing of chemical exchange-relayed NOEs in NMR experiments for the observation of protein–water interactions, *J. Magn. Reson.* **136,** 214–218 (1999).
26. A. J. Wand, D. L. Di Stefano, Y. Q. Feng, H. Roder, and S. W. Englander, Proton resonance assignments of horse ferrocytochrome c, *Biochemistry* **28,** 186–194 (1989).
27. Y. Q. Feng, H. Roder, S. W. Englander, A. J. Wand, and D. L. Di Stefano, Proton resonance assignments of horse ferricytochrome c, *Biochemistry* **28,** 195–203 (1989).
28. Y. Q. Feng, H. Roder, and S. W. Englander, Assignment of paramagnetically shifted resonances in the ^{1}H NMR spectrum of horse ferricytochrome c, *Biophys. J.* **57,** 15–22 (1990).
29. Y. Q. Feng, H. Roder, and S. W. Englander, Redox dependent structure change and hyperfine nuclear magnetic resonance shifts in cytochrome c, *Biochemistry* **29,** 3494–3504 (1990).
30. P. X. Qi, R. A. Beckman, and A. J. Wand, Solution structure of horse heart ferricytochrome c and detection of redox-related structural changes by high-resolution ^{1}H NMR, *Biochemistry* **35,** 12275–12286 (1996).
31. P. X. Qi, D. L. Di Stefano, and A. J. Wand, Solution structure of horse heart ferrocytochrome c determined by high-resolution NMR and restrained simulated annealing, *Biochemistry* **33,** 6408–6417 (1994).
32. L. Banci, I. Bertini, H. B. Gray, C. Luchinat, T. Reddig, A. Rosato, and P. Turano, Solution structure of oxidized horse heart cytochrome *c*, *Biochemistry* **36,** 9867–9877 (1997).
33. L. Banci, I. Bertini, J. G. Huber, G. A. Spyroulias, and P. Turano, Solution structure of reduced horse heart cytochrome c, *JBIC* **4,** 21–31 (1999).
34. G. W. Bushnell, G. V. Louie, and G. D. Brayer, High-resolution three-dimensional structure of horse heart cytochrome c, *J. Mol. Biol.* **214,** 585–595 (1990).
35. D. S. Cohen and G. J. Pielak, Entropic stabilization of cytochrome c upon reduction, *J. Am. Chem. Soc.* **117,** 1675–1677 (1995).
36. I. Bertini, C. Dalvit, J. G. Huber, C. Luchinat, and M. Piccioli, ePHOGSY experiment on a paramagnetic protein: Location of the catalytic water molecule in the heme crevice of the oxidized form of horse heart cytochrome c, *FEBS Lett.* **415,** 45–48 (1997).
37. L. Banci, S. Berners-Price, I. Bertini, V. Clementi, C. Luchinat, G. A. Spyroulias, and P. Turano, Water–protein interaction in native and partially unfolded equine cytochrome c (dedicated to Prof. R. Ernst), *Mol. Phys.* **95,** 797–808 (1998).
38. C. Dalvit, Homonuclear 1D and 2D NMR experiments for the observation of solvent–solute interactions, *J. Magn. Reson. Ser. B* **112,** 282–288 (1996).
39. C. Dalvit and U. Hommel, Sensitivity-improved detection of protein hydration and its extension to the assignment of fast-exchanging resonances, *J. Magn. Reson. Ser. B* **109,** 334–338 (1995).
40. C. Dalvit and U. Hommel, New pulsed field gradient NMR experiments for the detection of bound water in proteins, *J. Biomol. NMR* **5,** 306–310 (1995).
41. M. Piotto, V. Saudek, and V. Sklenar, Gradient-tailored excitation for single quantum NMR spectroscopy of aqueous solutions, *J. Biomol. NMR* **2,** 661–666 (1992).
42. V. Sklenar, M. Piotto, R. Leppik, and V. Saudek, Gradient-tailored water suppression for ^{1}H–^{15}N HSQC experiments optimized to retain full sensitivity, *J. Magn. Reson. Ser. A* **102,** 241–245 (1993).

43. A. G. Sobol, G. Wider, H. Iwai, and K. Wüthrich, Solvent magnetization artifacts in high-field NMR studies of macromolecular hydration, *J. Am. Chem. Soc.* **130,** 262–271 (1998).

44. D. Marion and K. Wüthrich, Application of phase-sensitive correlated spectroscopy (COSY) for measurements of proton–proton spin–spin coupling constants in proteins, *Biochem. Biophys. Res. Commun.* **113,** 967–974 (1983).

45. S. Macura and R. R. Ernst, Elucidation of cross relaxation in liquids by two-dimensional NMR spectroscopy, *Mol. Phys.* **41,** 95–95 (1980).

46. T. L. Hwang, S. Mori, A. J. Shaka, and P. C. M. van Zijl, Application of phase-modulated CLEAN chemical EXchange Spectroscopy (CLEANEX-PM) to detect water–protein proton exchange and intermolecular NOEs, *J. Am. Chem. Soc.* **119,** 6203–6204 (1998).

47. S. Mori, J. Berg, and P. C. M. van Zijl, Separation of intramolecular NOE and exchange peaks in water exchange spectroscopy using spin echo filters, *J. Biomol. NMR* **7,** 77–82 (1996).

48. G. Wider, R. Riek, and K. Wüthrich, Diffusion filters for separation of solvent–protein and protein–protein nuclear Overhauser effects (HYDRA), *J. Am. Chem. Soc.* **118,** 11629–11634 (1996).

49. D. S. Wishart, B. D. Sykes, and F. M. Richards, Relationship between nuclear magnetic resonance chemical shift and protein secondary structure, *J. Mol. Biol.* **222,** 311–333 (1991).

50. A. Böckmann, F. Penin, and E. Guittet, Rapid estimation of relative amide proton exchange rates of ^{15}N-labeled proteins by a straightforward water selective NOESY-HSQC experiment, *FEBS Lett.* **383,** 191–195 (1996).

51. S. Mori, C. Abeygunawardana, and P. C. M. van Zijl, Water exchange filter with improved sensitivity (WEX II) to study solvent-exchangeable protons. Application to the consensus zinc finger peptide CP-1, *J. Magn. Reson. Ser. B* **110,** 96–101 (1996).

52. Y. W. Bai, J. S. Milne, L. Mayne, and S. W. Englander, Primary structure effects on peptide group hydrogen exchange, *Proteins Struct. Funct. Genet.* **17,** 75–86 (1993).

53. N. R. Krishna, K. P. Sarathy, D.-H. Huang, R. L. Stephens, J. D. Glickson, C. W. Smith, and R. Walter, Primary amide hydrogen exchange in model amino acids: Asparagine, glutamine, and glycine amides, *J. Am. Chem. Soc.* **104,** 5051–5053 (1982).

54. T. L. Hwang, P. C. M. van Zijl, and S. Mori, Accurate quantification of water–amide proton exchange rates using the Phase-Modulated CLEAN chemical EXchange (CLEANEX-PM) approach with a Fast-HSQC (FHSQC) detection scheme, *J. Biomol. NMR* **11,** 221–226 (1998).

55. L. Banci, G. Gori Savellini, and P. Turano, A molecular dynamics study in explicit water of the reduced and oxidized forms of yeast iso-1-cytochrome c. Solvation and dynamic properties of the two oxidation states, *Eur. J. Biochem.* **249,** 716–723 (1997).

56. A. M. Berghuis and G. D. Brayer, Oxidation state-dependent conformational changes in cytochrome c, *J. Mol. Biol.* **223,** 959–976 (1992).

57. H. Ochi, Y. Hata, N. Tanaka, M. Kakudo, T. Sakuri, S. Achara, and Y. Morita, Structure of rice ferricytochrome c at 2.0 A resolution, *J. Mol. Biol.* **166,** 407–418 (1983).

58. T. Takano and R. E. Dickerson, Conformation change of cytochrome c: I. Ferrocytochrome c structure refined at 1.5 Å resolution, *J. Mol. Biol.* **153,** 79–94 (1981).

59. T. Takano and R. E. Dickerson, Conformation change in cytochrome c: II. Ferricytochrome c refinement at 1.8 Å and comparison with ferrocytochrome c structure, *J. Mol. Biol.* **153,** 95–155 (1981).

60. G. V. Louie and G. D. Brayer, High-resolution refinement of yeast iso-1-cytochrome c and comparison with other eukaryotic cytochromes, *J. Mol. Biol.* **214,** 527–555 (1990).

61. V. P. Denisov, B. Halle, J. Peters, and H. D. Horlein, Residence times of the buried water molecules in bovine pacreatic trypsin inhibitor and its G36S mutant, *Biochemistry* **34,** 9046–9051 (1995).

62. V. P. Denisov, J. Peters, H. D. Horlein, and B. Halle, Using buried water molecules to explore the energy landscape of proteins, *Nature Struct. Biol.* **3,** 505–509 (1996).

63. G. D. Brayer and M. E. P. Murphy, Structural studies of eukariotic cytochromes *c*, *in* "Cytochrome *c*. A Multidisciplinary Approach" (R. A. Scott and A. G. Mauk, Eds.), pp. 103–166, University Science Books, Sausalito, CA (1996).

64. R. Koradi, M. Billeter, and K. Wüthrich, MOLMOL: A program for display and analysis of macromolecular structure, *J. Mol. Graphics* **14,** 51–55 (1996).